Addendum to Report 109

November, 1957.

THE COLLEGE OF AERONAUTICS

CRANFIELD

Addendum to College of Aeronautics Report 109:

A Theoretical and Experimental Study of the Boundary Layer Flow on a 45° Swept Back Wing.

by

J. Walton

(Prepared under Ministry of Supply Contract No. 6/Aircraft/14002/C.B.6(a)

SUMMARY

College of Aeronautics Report 109 (Ref.1) describes Flight Tests carried out on a swept back half wing of double elliptic section to investigate the nature of the boundary layer flow, with particular reference to Bounday Layer Instability and subsequent transition.

The wing, which had a chord of 7ft.2" was mounted as a dorsal fin on the mid upper fuselage of an Avro Lancaster, which enabled a Reynolds Number range of 0.88×10^6 - 1.92×10^6 per foot to be achieved. There was some doubt about the validity of applying the results of these tests to wings of orthodox section because of the possible occurrence of wake instability associated with the bluff trailing edge. This Addendum gives the results of a few check tests on the same wing with a short trailing edge extension having a trailing edge angle of approximately 12°. Unfortunately wing surface deterioration near the L.E. from mid semi span to the tip prevented conclusive results being obtained but some evidence is presented to show that the results of Ref. 1 are not invalidated by the choice of section.

CONTENTS

CONTENTS (contd.)

1. INTRODUCTION

Ref. 1 describes the experiments made to investigate the nature of the boundary layer flow with particular reference to sweep instability on a swept back half wing in flight. The wing which had a semi span of 8'6.5", a constant chord of 7'2" and a sweep back of 45° was mounted as a dorsal fin on the mid fuselage of an Avro Lancaster which enabled a Reynolds Number Range (based on 86" chord) of $6.4 \times 10^6 - 13.7 \times 10^6$ to be obtained. The wing section was formed by two semi ellipses having a common minor axis of 13" at the maximum thickness, the fore and aft parts having semi major axes of 52" and 34" respectively.

The main conclusions of Ref. 1 may be summarised as follows ;

(1) The use of the aircraft as a test vehicle was perfectly satisfactory.

(2) The conditions for instability of the secondary flow are given by an equation of the type

$$\frac{x_{max}}{R^{\frac{1}{2}}} = \frac{N}{R^{\frac{1}{2}}_{crit}} \quad , \quad 120 < N < 160.$$

(3) The measured pressure distributions were in close agreement with calculations based on the infinite sheared wing and an equivalent source distribution for the zero incidence case (symmetrical section).

(4) Tuft observations showed that for both upper and lower surfaces within the incidence range $0^{\circ} - 10^{\circ}$, three dimensional effects did not achieve first order importance, thus permitting the use of strictly two dimensional techniques for boundary layer measurements.

(5) No laminar flow was detected on either wing surface at Reynolds Numbers of 10.85×10^6 or above nor at incidences of 60° or above.

The reasons for using a double elliptic section were given in Ref.1 para. 2.1 and may be briefly restated as follows :-

The three dimensional boundary layer instability phenomena requires a study of the flow over and near to the leading edge of the wing at full scale Reynolds Numbers. Consequently if it is supposed that the flow in this region can be simulated by using a section with a foreshortened trailing edge representing a wing of much longer chord it is then possible to build a test wing with a much larger distance between the leading edge and maximum thickness for the same actual wing area. Such a wing would enable much higher Reynolds Numbers (based on the distance from L.E. to max. thickness) to be obtained for the same max. permissible loading than a wing of orthodox section. Thus the design of wing of Ref. 1 was based on this assumption with an actual chord of 86" which, it was suggested, was representative of an orthodox wing with a chord of 130". The latter dimension was referred to as the "effective" chord in Ref. 1.

In Ref. 1 paras. 2.1 and 2.3 the author uses the experimental and theoretical results to show that the above argument is erroneous as far as the simulation of flow conditions is concerned. It is pointed out that this does not invalidate the results but means that they may be compared to those on wings having similar pressure distributions.

In para. 2.1 it is also pointed out that no trace of wake instability due to the bluff trailing edge was detected. It was the intention in this note to show positively whether or not wake instability was encountered and in order to do so, a short V-section trailing edge extension was fitted to the wing of Ref. 1 and a few checktests were made under the same conditions as thoseof Ref. 1.

2. EXPERIMENTAL EQUIPMENT

2.1. The Aircraft

The aircraft used for the tests of Ref. 1 (Avro Lancaster Mk.7 PA-474) was used as the test vehicle for the present tests without further modification.

2.2. The Test Wing

The test wing of Ref. 1 was modified by the attachment of a trailing edge extension of light alloy skin stiffened by 7 light alloy ribs as described in Ref. 2. The above extension increased the actual chord of the wing by 24" from 86" to 110" as shown in Figs. 3 and 4 and had a trailing edge angle of 12°. Five static pressure tapping holes flush with the skin surface at approximately mid semi-span were built into the extension.

The reason for not fairing the extension into the basic wing to give a smooth contour was that the boundary layer was already turbulent well forward of the proposed wing extension juncture and it was considered that the slight concavity in the wing contour would not affect the flow forward of the maximum thickness, beyond which laminar flow had not been detected.

The Boundary Layer Fence at the root was extended rearwards approximately 18".

Table 1 compares the various geometric features of the wing with and without the trailing edge extension.

The Chordwise rows of static pressure tappings with 13 tappings in each row were on the port side only. These were at spanwise positions of $y/s = 0.223$, 0.497 and 0.772 measured from the boundary layer fence. The chordwise positions of each tapping is given in Table 2. As the wing section was symmetrical negative incidence results may be taken as lower surface values. The same applies to the boundary layer measurements which were made on the starboard side only, at the same spanwise positions.

Before the present flight tests were begun, it was noticed that the wing surface had seriously deteriorated on both surfaces near the tip and had slightly deteriorated at about mid semi-span. Nearer the root, the wing surface was not affected. The above deterioration appeared to be due to the filling in the joint (approx. 5.65" from the leading edge) between the mahogany leading edge member and the light alloy skin, being forced out and lifting the cellulose finish. This was most probably due to temperature and humidity variations between the two series of tests. The wing surface was refinished, and checked by a strip light as described in Ref. 1 para.4.3, but no measurements of the surface roughness or waviness could be made as all the work had to be carried out with the wing mounted on the aircraft. Unfortunately the present series of tests showed that the attempted restoration was not completely successful and that further deterioration took place during the tests.

2.3. Instrumentation.

The manometer, F.24 camera installation and yawmeter were used without alteration as described in Ref. 1 paras. 4.4 and 4.5 except that water (with a purple dye) was used as the manometric fluid. For the last flight of the series a pitot-in-venturi was installed on the starboard side of the fuselage symmetrically opposite the standard aircraft pitot head on the port side and a 0 - $\pm$ 2" Differential Pressure Gauge mounted on the pilot's combing was connected between the two pitots.

2.4. Boundary Layer Combs and Transition Indicators

These were exactly as described in Ref. 1 para.4.6.

2.5. Pressure Leads.

The pressure leads from the boundary layer combs and transition indicators differed from those used previously (see Ref. 1 para.4.7) in two respects. The 10 tube P.V.C. "tube tape" was dispensed with, thus eliminating several joints in each lead and the 3 mm O.D. neoprine

tubing was taken direct from the boundary layer combs and T.I's into the fuselage and thence via a short length of $\frac{1}{4}$" O.D. rubber tubing to the manometer. As before, the leads were made long enough to traverse to the leading edge but the excess was coiled and stored in the fuselage. To reduce to a minimum the interference of the pressure leads with the airflow over the wing, the tubing was taken as far aft as possible and thence down the concavity at the joint between the basic wing and the trailing edge extension, over the aftmost point of the boundary layer fence, and into the fuselage. It was found convenient to form the 13 neoprine leads from each boundary layer comb into groups by sellotape straps at about 12" intervals along their lengths. The attachment of the boundary layer combs, T.I's and the pressure leads to the wing was done entirely with sellotape and finally the "leading edge" of the tubing running down the wing (spanwise) and faired over with sellotape.

3. DETAILS OF TESTS

The static pressure distribution over the basic wing previously measured was from the leading edge only to the maximum thickness, hence the static pressure over a large section of the wing was in doubt. Consequently the speed/incidence envelope of the test wing with the T.E. extension was more severely limited than for the tests of Ref. 1 see Fig. 6. However, this was of little consequence as it was possible to repeat all the conditions in which laminar flow had previously been detected.

Only four flights were possible before the aircraft was grounded for a major overhaul at which point the present tests were terminated. On the first flight the pressure distribution was obtained and on the subsequent three flights the boundary layer profiles and transition indicator readings were obtained at 39", 26" and 13" from the leading edge at the same spanwise positions as those of Ref. 1.

All tests were performed at 10,000' at 90 kts., 110 kts., and 158 kts., or maximum within the envelope with the test wing incidence varied by 2° increments each way. As before the above flight conditions

give Reynolds Number 0.88, 1.08 and 1.55 x 10^6 per ft.

As in Ref. 1 the boundary layer combs were traversed chordwise at the spanwise positions (measured from the boundary layer fence) given by y/s = 0.223, 0.497 and 0.772. The transition indicators were traversed chordwise at y/s = 0.086, 0.360, 0.635 and 0.909.

For the last flight the wing was extensively covered with wool tufts and observations were made from the D.H. Dove G-ALVF as described in Ref. 1 para. 5.5.

It had been noted that in both series of tests (e.g. Ref. 1, Fig. 34), the total head, at low speeds, measured outside the boundary layer on the wing was almost invariably higher than the free stream total head measured by the aircraft pitot system even when the static pressure error had been taken into account. Hence the a/c pitot pressure was checked by the instrumentation mentioned in para. 2.3 and the system was found to have quite a large pitot pressure error at low speeds, as shown in Fig. 5a.

4. PRESENTATION OF RESULTS

The method chosen to present the results is one that enables a direct comparison to be made with those results of Ref. 1 which were obtained under the same conditions. With this end in view, the layout of the experimental results closely follows that of Ref. 1; all full lines applying to the present results, all chained lines being the corresponding results of Ref. 1 unless otherwise stated. As the present tests apply to the wing with a greater chord than that of Ref. 1, for clarity all chordwise positions are given in terms of the distance x from the leading edge in the streamwise direction in inches. Any distance x may be easily converted into the percentage length of either chord by reference to Fig. 7.

Fig. 8 shows the mean chordwise pressure distribution from the leading edge to maximum thickness over the swept back half wing as obtained from the surface tappings. The C_p shown is the mean for three

speeds for $\alpha = 0 - \pm 6^{\circ}$, two speeds for $\alpha = \pm 8^{\circ}$ and the actual C_p for $\alpha = \pm 10^{\circ}$, at 90 kts. (R.N. = 0.88×10^6 per foot). For clarity the pressure distributions previously obtained (ref. 1 Fig. 25) are omitted. However, Fig. 9 compares the chordwise loading ΔC_p on a percentage of chord basis, i.e. the results of Ref. 1, Fig. 26, are plotted against x/c_o and the present results against x/c, a common scale being used for x/c_o and x/c.

Unfortunately no photographs of the tufts were obtained but Fig. 10 shows a sketch of the tuft pattern on the upper surface at 10° incidence based on the description of an observer in the Dove.

The velocity profiles are compared in Figs. 11 and 13 and transition fronts in Fig. 14.

5. DISCUSSION OF RESULTS

5.1. Static Pressure Distribution

When the results of Ref. 1 Fig. 25 are compared with those of Fig. 8 of the present note it is seen that, for all incidences except $+6$ and $+10^{\circ}$, the static pressure coefficient is, generally speaking, increased by about 0.02 over most of the chord by the addition of the trailing edge extension. This value is within the limits of accuracy of the experimental procedure as shown in Appendix 1 of Ref. 3. The slight decrease in static pressure at $\alpha = +6^{\circ}$ and $\alpha = +10^{\circ}$ is most likely due to the a/c having had a small angle of sideslip which would increase the incidence of the wing.

The chordwise loading graphs are more informative and when plotted against the distance x show that the loading is moved slightly aft with the trailing edge extension. This is, of course, what might be expected considering the simple assumption that the pressure distribution on an aerofoil section at incidence α is obtained from the sum of the pressures on the section at zero incidence plus a flat plate at incidence α. When plotted as in Fig. 9 it is shown that the trailing edge of the basic wing section of Ref. 1 is well defined; the effective

trailing edge being, in fact, approximately 4% c_o behind the actual trailing edge.

5.2. Tuft Observations

Although the sketch of the tuft pattern shown in Fig. 10 is only qualitative as suggested in para. 4, particularly in the region of the trailing edge extension, it is seen that the flow is approximately chordwise in the region in which boundary layer measurements were made. Hence the use of the boundary layer combs which strictly are for use in two dimensional flow only, is not invalidated.

5.3. Boundary Layer Measurements

It is immediately apparent from the velocity profiles, Figs. 11 - 13, that at the tip and mid semi-span stations transition occurred further forward in the present tests than in those of Ref. 1 due to the reasons given in para. 2.2. At the root station, transition appears, in general, to be slightly delayed by the addition of the trailing edge extension. The agreement between the turbulent profiles of Ref. 1 and the present note is in accordance with the observations that, on a flat plate, the thickness of the turbulent boundary layer is dependent on the distance from the stagnation line and not on the point of transition. The above agreement also shows that experimental conditions can be consistently reproduced to a high degree of accuracy with the present technique.

From an examination of the velocity profiles it will be seen that, near the surface, the heights at which the measured velocity ratios have been plotted do not correspond with the nominal tube heights given in Ref. 1 Fig. 13. The reason for this is that in general it was not found possible to draw a smooth set of profiles using the nominal tube heights and consequently they were measured on each comb at each chordwise position.

5.4. Shape Parameter and Boundary Layer Transition

As only three chordwise positions of the surface total head distribution were available, it was not possible to obtain a complete picture of the boundary layer transitions by the same method as in Ref. 1. This method used the total head rise shown by a creeping surface pitot when passing from a laminar boundary layer to a turbulent one, although in some cases this total head rise was not well defined.

However, by plotting the Shape Parameter H against x for the velocity profiles of Ref. 1 clearly defined curves were obtained and taking the end of the transition region to be the point where H attained a steady value (approximately 1.5, the value for a turbulent boundary layer) it was possible to redetermine the transition points for the original wing with more certainty. These points which as in Ref. 1, were taken to be the end of the transition region, were in general in good agreement with those of Ref. 1, Fig. 35 which were mainly determined from total head measurements. Then, assuming that the curves of H ~ x for each incidence and speed would be similar, over a small region, for the wing with or without the extension, the above curves were given a small chordwise displacement to pass through the points for the wing with the extension, and hence the transition points for the wing with the extension were found.

Using a similar technique for the total head measurements of the transition indicators, the transition fronts for $R = 0.88 \times 10^6$/ft. shown in Fig. 14 were determined. For consistency the transition fronts shown for the original wing are those redetermined by the shape parameter method. No fronts for $R = 1.08 \times 10^6$/ft are shown as transition appeared in general to be ahead of x = 13", the most forward position at which measurements were made with the trailing edge extension.

6. CONCLUSIONS

While the tests described herein were not conclusive due to the short time available and to surface deterioration towards the wing tip, there is sufficient evidence to suggest that the trailing edge of the swept back half wing of double elliptic section, described in Ref. 1, was in fact fairly well defined and was not likely to have given rise to wake instability.

It is therefore suggested that the results of Ref. 1 may well be representative of similar wings with orthodox sections.

In general transition movements over the forward part of the wing do not appear to be unduly influenced by the shape of the fairing aft of the maximum thickness to the trailing edge.

REFERENCES

1.	Burrows, F.M.	A Theoretical and Experimental Study of the Boundary Layer Flow on a 45° Swept Back Wing. College of Aeronautics Report No.109.
2.	Department of Aircraft Design. C. of A.	Supplement to Addendum to Type Record Avro Lancaster PA.474. College of Aeronautics, 1956.
3.	Burrows, F.M.	Characteristics of the flow field over the mid upper fuselage of Lancaster PA.474.

SYMBOLS

s	Semi span of test wing (B.L.Fence to tip)
c_o	chord of original wing
c	chord of wing with T.E. extension
x	distance along chord from L.E.
y	distance spanwise from B.L. Fence
R	Reynolds Number
x	Secondary Flow Reynolds Number
α	Geometric wing incidence

TABLE 1

Comparison of the Geometric Particulars of the wing, without and with the trailing edge extension.

	Without Extension (as in Ref.1)	With Extension (as in present note)
Semi-Span (From B.L. Fence to Tip)	87.5"	87.5"
Chord	86"	110"
Wing Area of Half Wing (Outboard of B.L.Fence)	52.257 sq.ft.	66.84 sq.ft.
Aspect Ratio	2.035	1.591
Taper Ratio	1	1
Max. Thickness	13"	13"
Thickness/Chord Ratio	0.151	0.118
Distance to Max.Thickness from L.E. along chord	52"	52"
Distance to Max. Thickness as % of chord	60.5	47.25

TABLE 2

The position of static pressure tappings in the swept back half wing.

Spanwise positions : y/s = 0.223, 0.497 & 0.772

Hole No.	Distance from L.E. along chord inches	$\frac{x}{c_o}$ %	$\frac{x}{c}$ %
1	0	0	0
1a	0.325	0.378	0.296
1b	0.650	0.756	0.591
1c	0.975	1.135	0.887
2	1.3	1.512	1.183
3	2.6	3.03	2.365
4	5.2	6.04	4.73
5	7.8	9.06	7.095
6	10.4	12.10	0.45
7	13	15.12	11.83
8	19.5	22.70	17.72
9	26	30.25	23.65
10	32.5	37.80	29.55
11	39	45.40	35.45
12	45.5	52.9	41.3
13	50.6	58.8	46

Holes numbered 1a, b and c were in the neoprine tubing let into the leading edge, see Ref. 1, para. 4.3. Each hole was used in turn and then filled with beeswax.

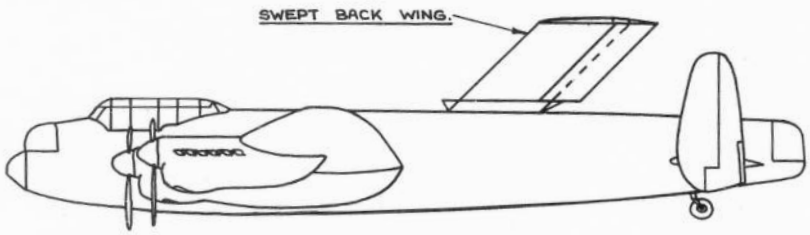

FIG. 1 . ARRANGEMENT OF AIRCRAFT & WING.

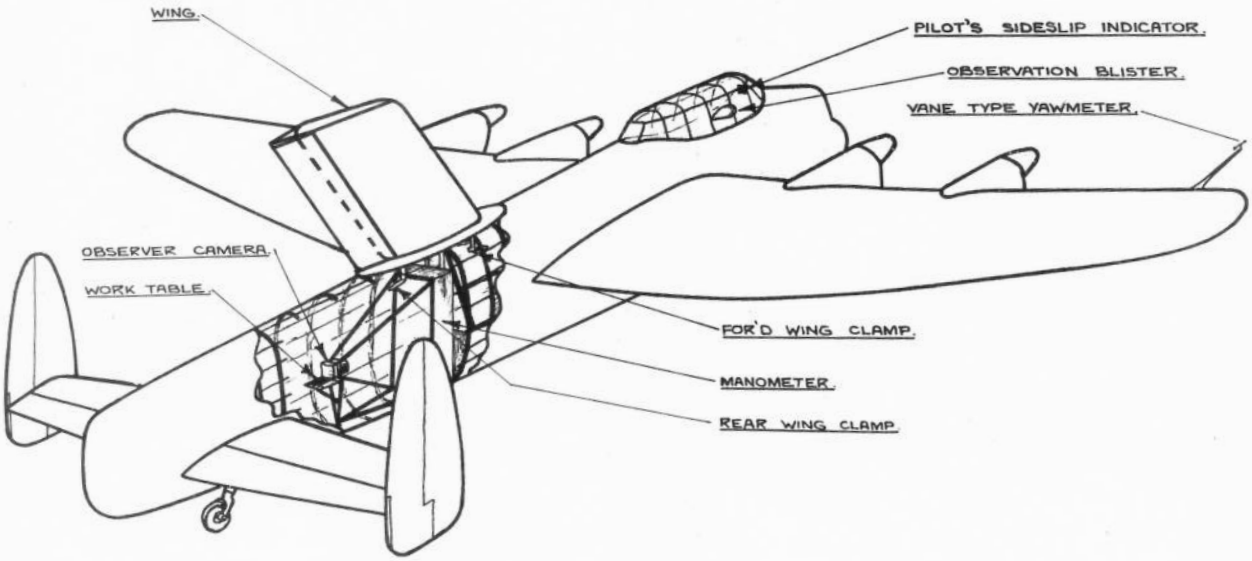

FIG.2. LAYOUT OF EQUIPMENT IN AIRCRAFT.

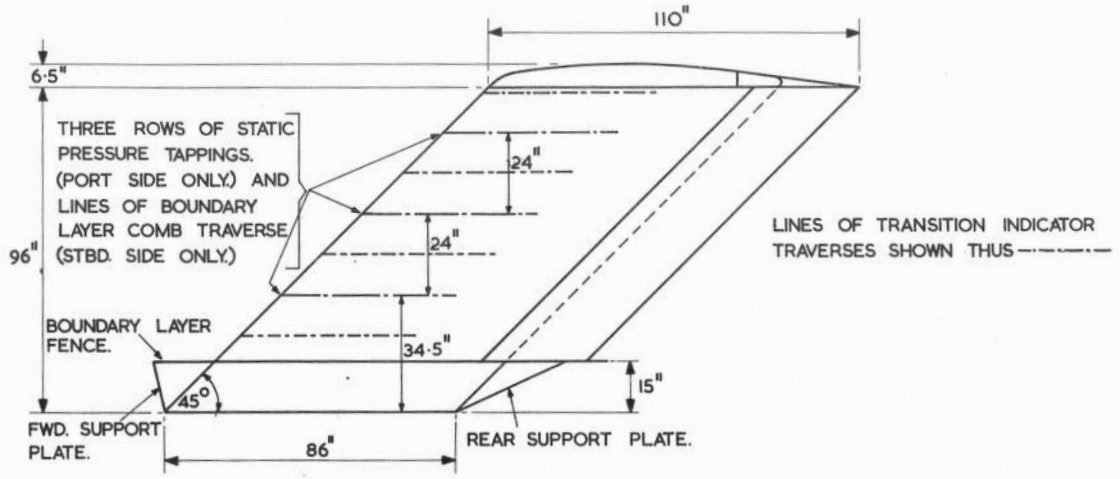

FIG. 3. PLANFORM OF SWEPT BACK HALF WING.

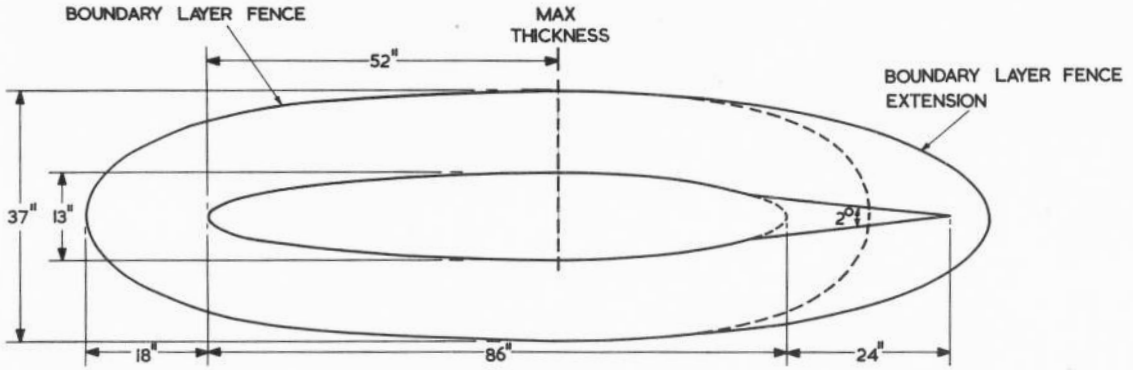

FIG. 4. SECTION OF SWEPT BACK HALF WING.

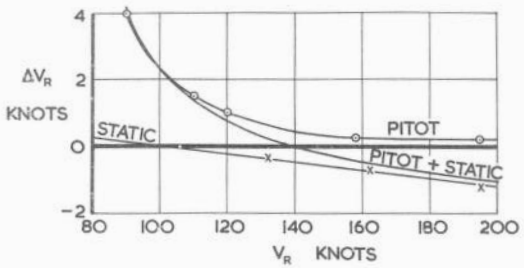

FIG. 5a. PRESSURE ERROR CORRECTION CURVES FOR LANCASTER P.A. 474

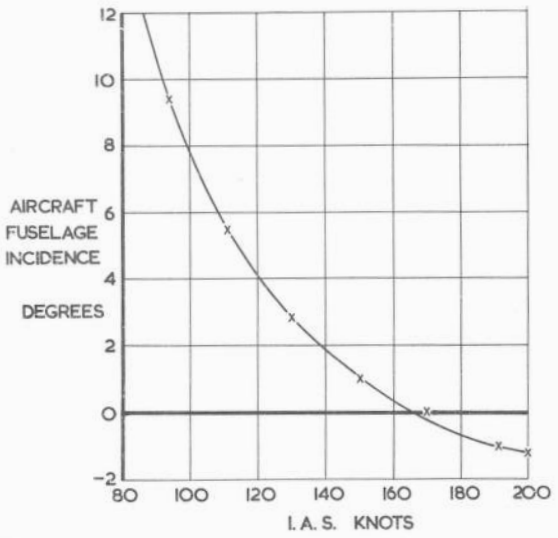

FIG. 5b. VARIATION OF AIRCRAFT FUSELAGE INCIDENCE WITH SPEED AT 44,000 lb A.U.W.

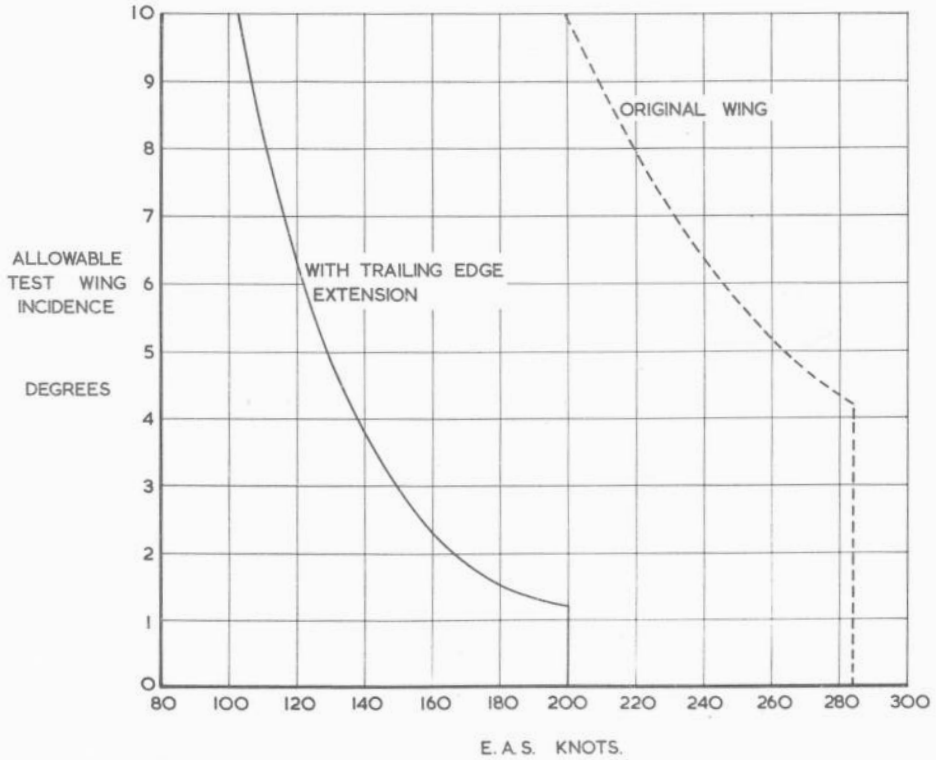

FIG. 6. AIRCRAFT SPEED—TEST WING INCIDENCE ENVELOPE.

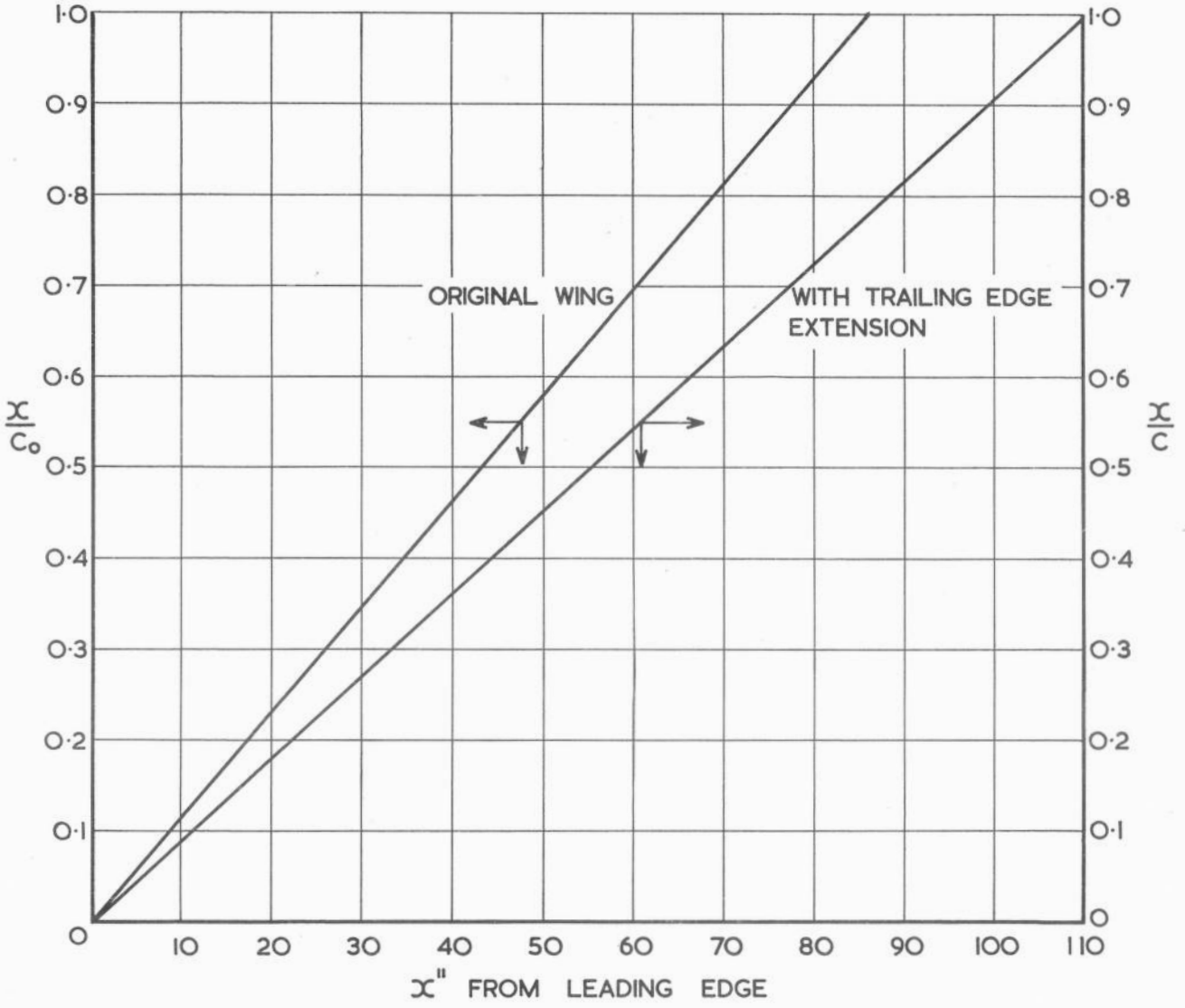

FIG. 7. DISTANCE FROM LEADING EDGE AS A PERCENTAGE OF CHORD.

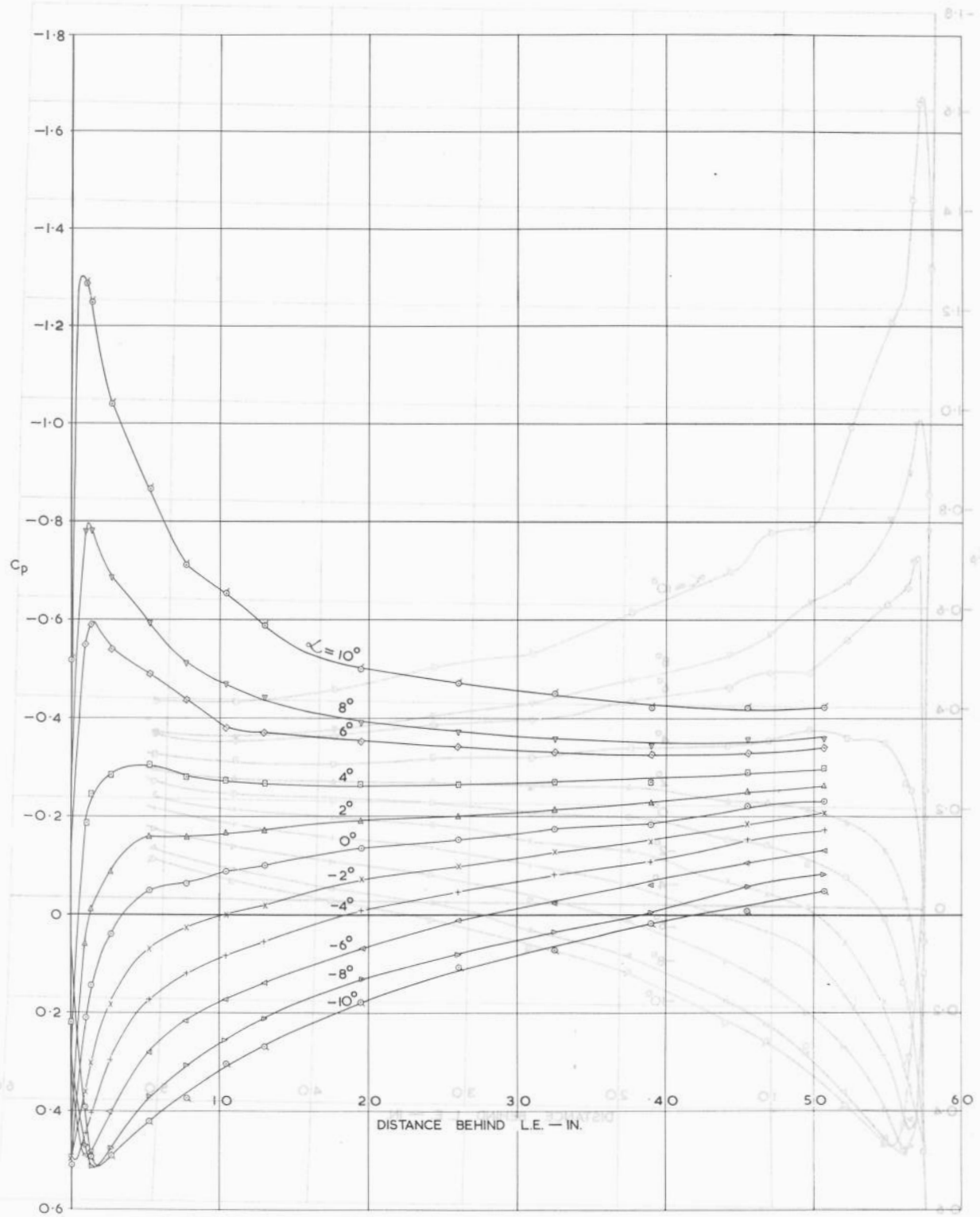

FIG. 8a. MEAN STATIC PRESSURE DISTRIBUTION

$R = 0{\cdot}88 \times 10^6 - 1{\cdot}55 \times 10^6$ /FT.

$\frac{y}{s} = 0{\cdot}223$

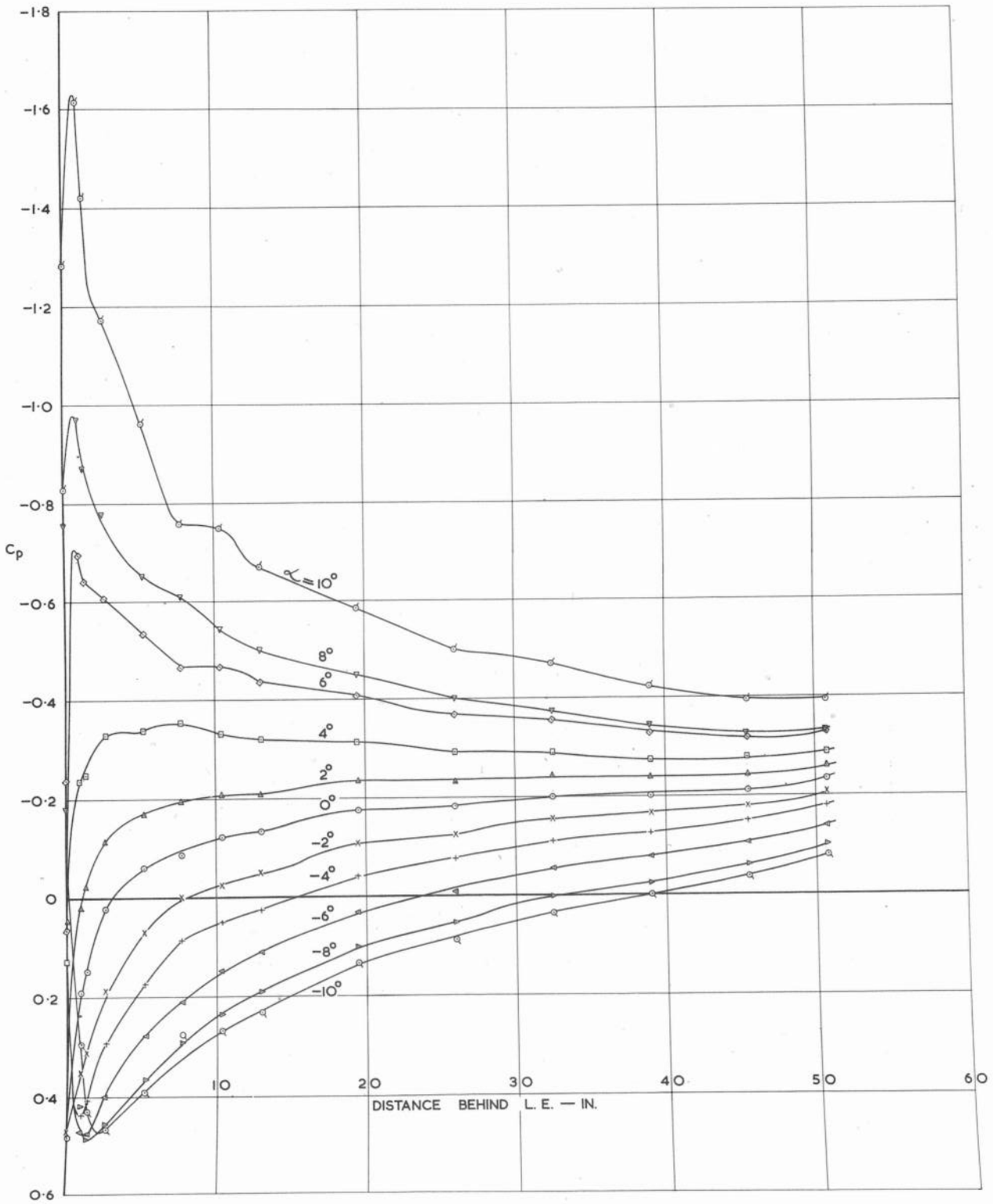

FIG. 8b. MEAN STATIC PRESSURE DISTRIBUTION

$R = 0{\cdot}88 \times 10^6 - 1{\cdot}55 \times 10^6$/FT.

$\frac{y}{s} = 0{\cdot}497$

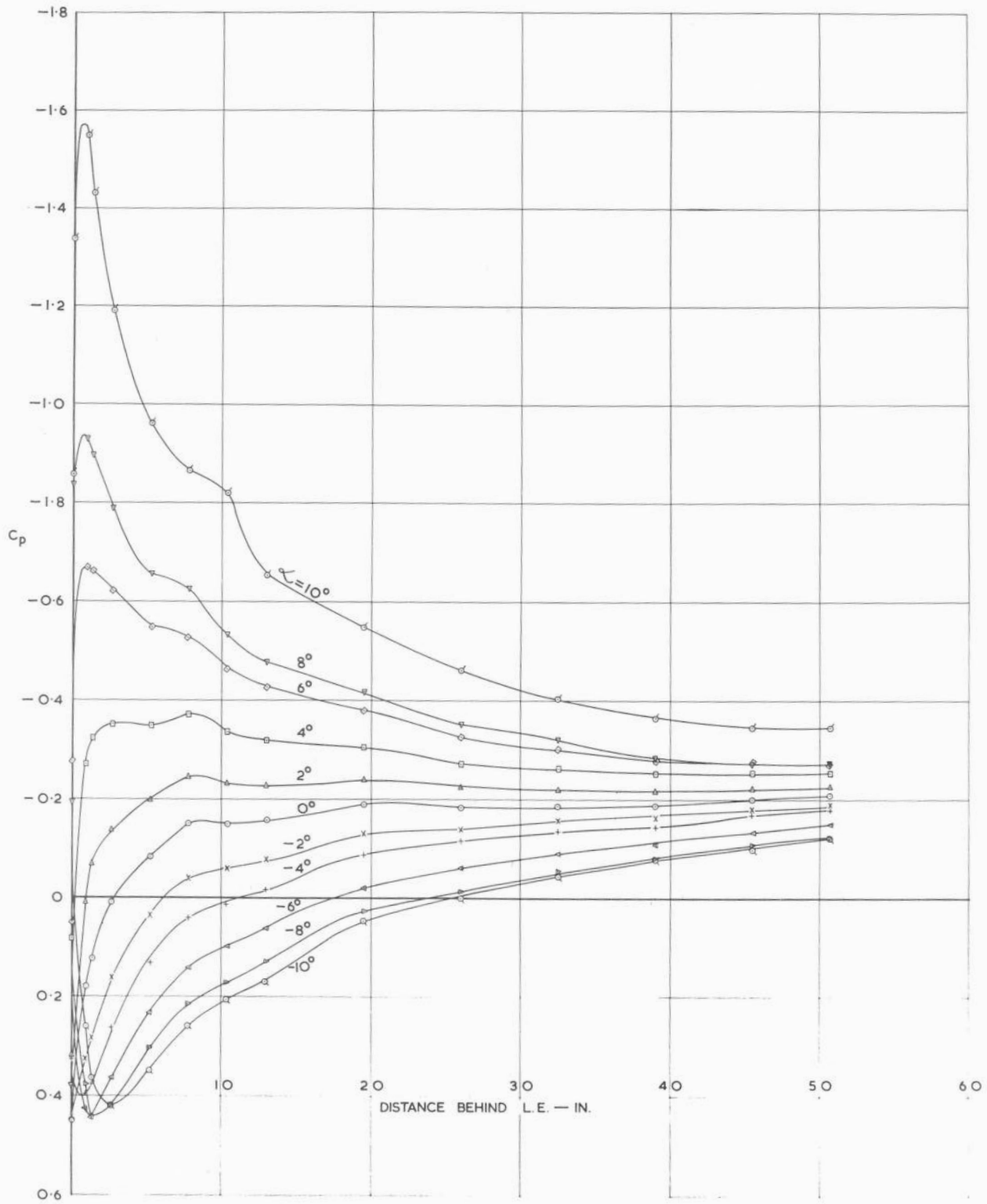

FIG. 8c. MEAN STATIC PRESSURE DISTRIBUTION

$R = 0{\cdot}88 \times 10^6 - 1{\cdot}55 \times 10^6$/FT

$\frac{y}{s} = 0{\cdot}772$

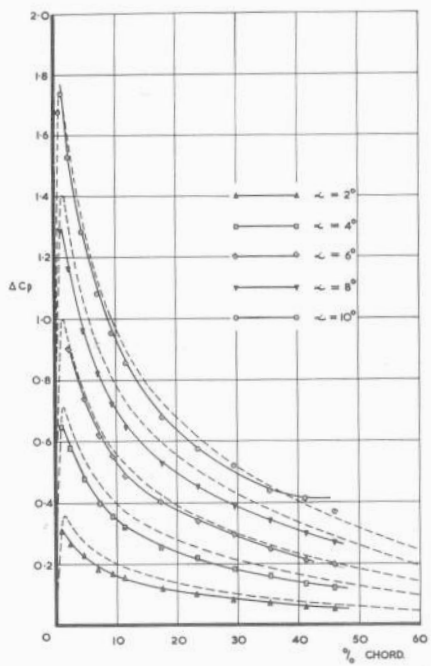

$\frac{y}{s} = 0.223$

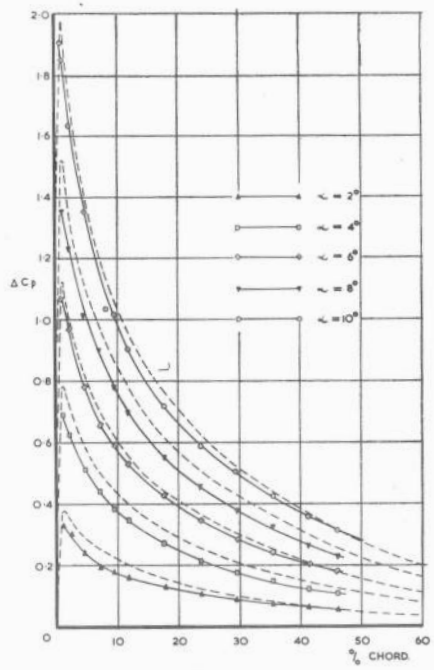

$\frac{y}{s} = 0.497$

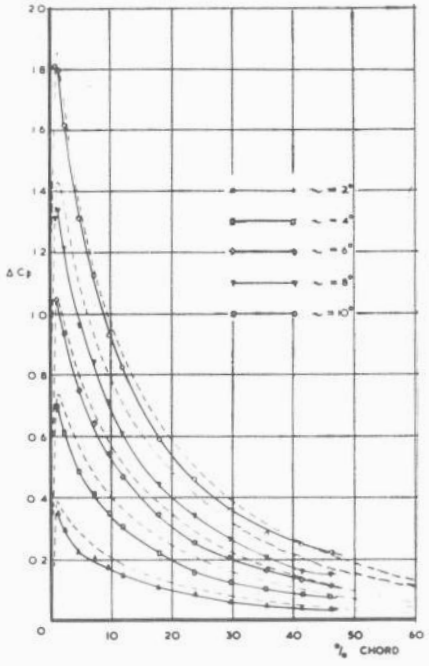

$\frac{y}{s} = 0.772$

$R = 0.88 \times 10^6 - 1.55 \times 10^6$/FT

FIG. 9. MEAN CHORDWISE LOADINGS.

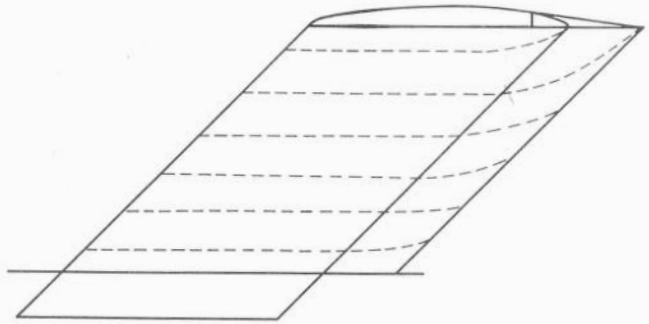

FIG. 10. TUFT OBSERVATIONS UPPER SURFACE
$\alpha = 10°$

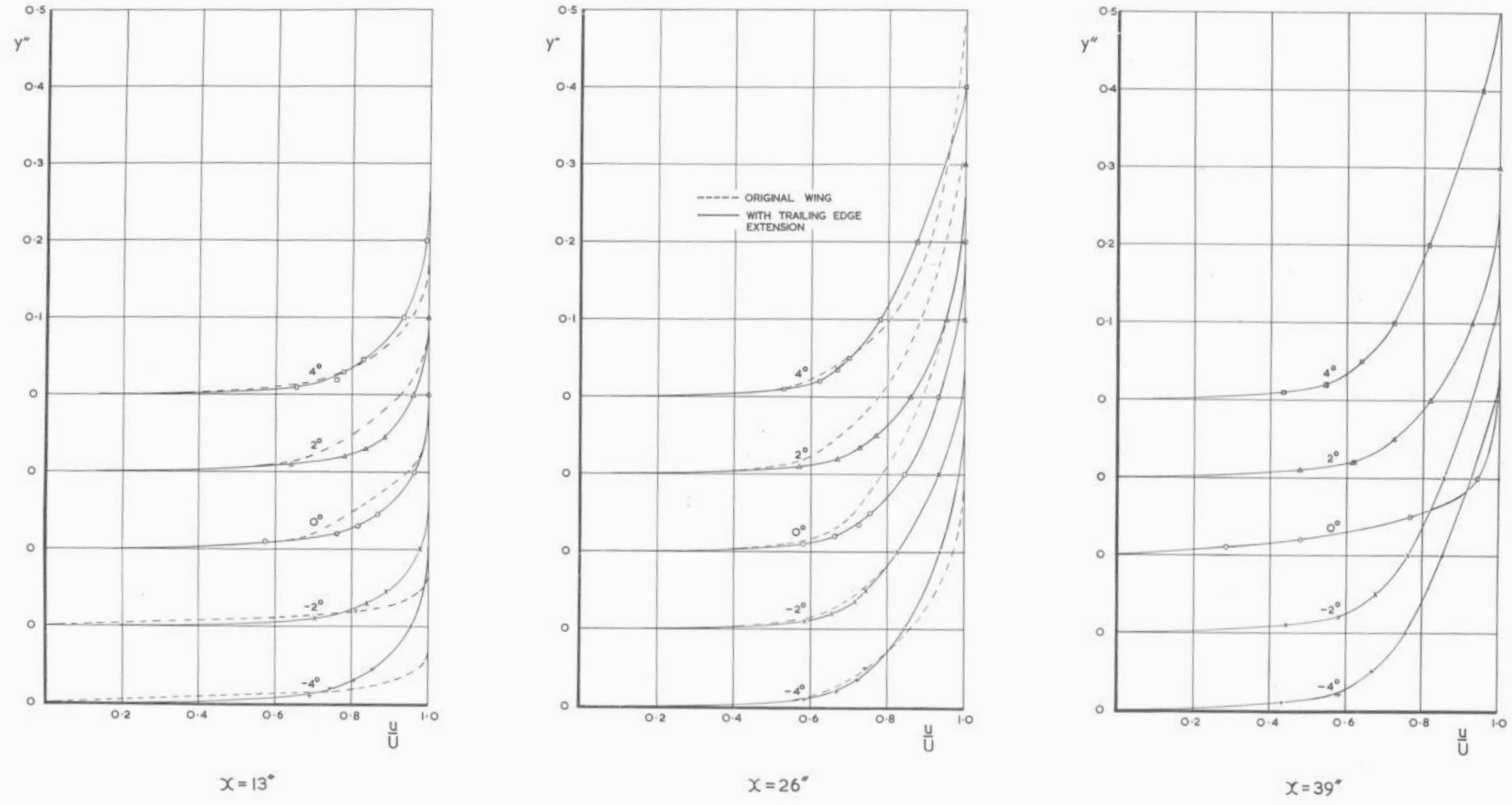

(a) $R = 0{\cdot}88 \times 10^6$/FT.

FIG. 11. BOUNDARY LAYER VELOCITY PROFILES. $y/s = 0{\cdot}223$

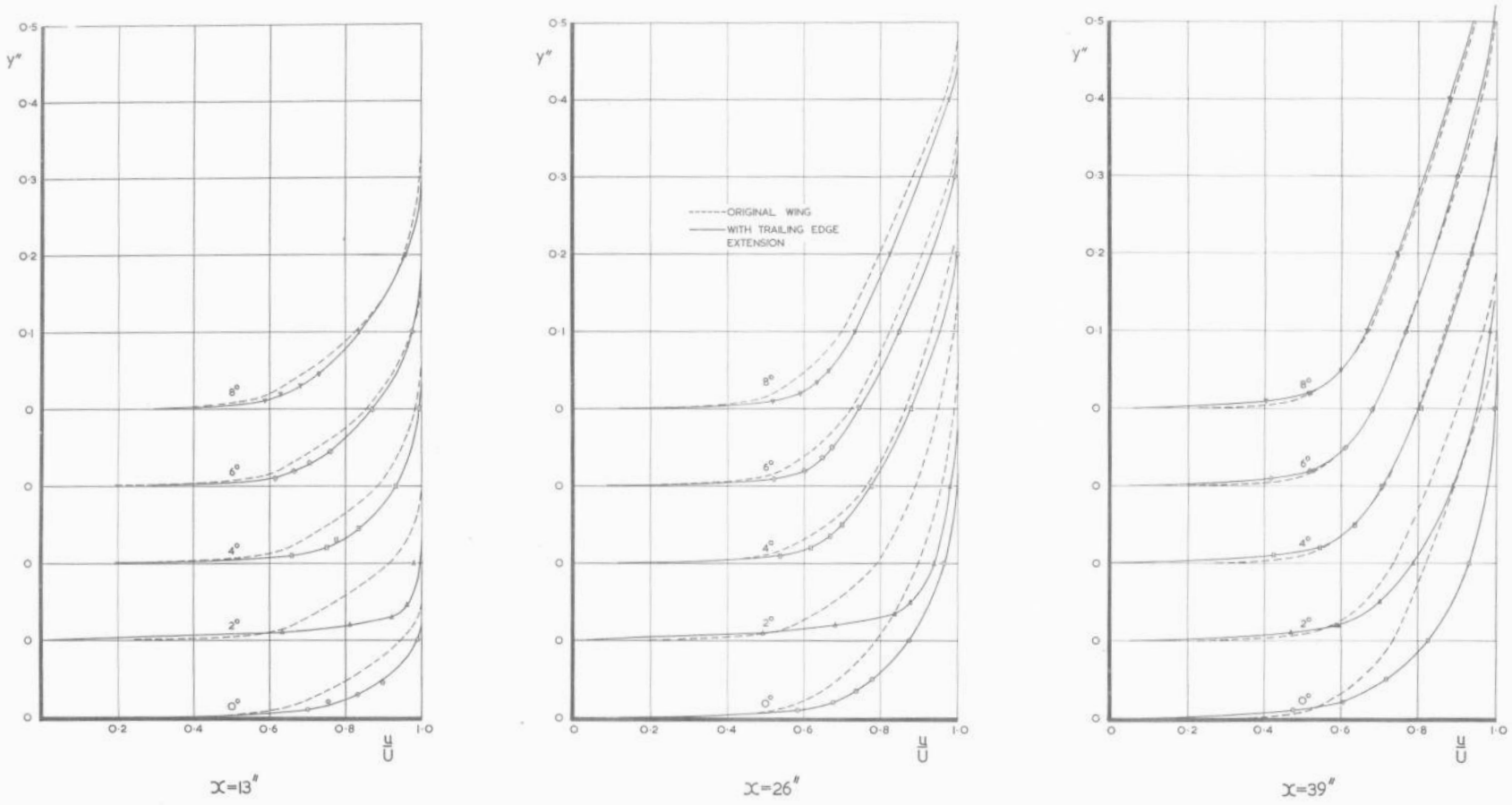

(b.) $R = 1{\cdot}08 \times 10^6$/FT.
$\alpha = 0° - 8°$

FIG. 11. BOUNDARY LAYER VELOCITY PROFILES. $y/s = 0{\cdot}223$

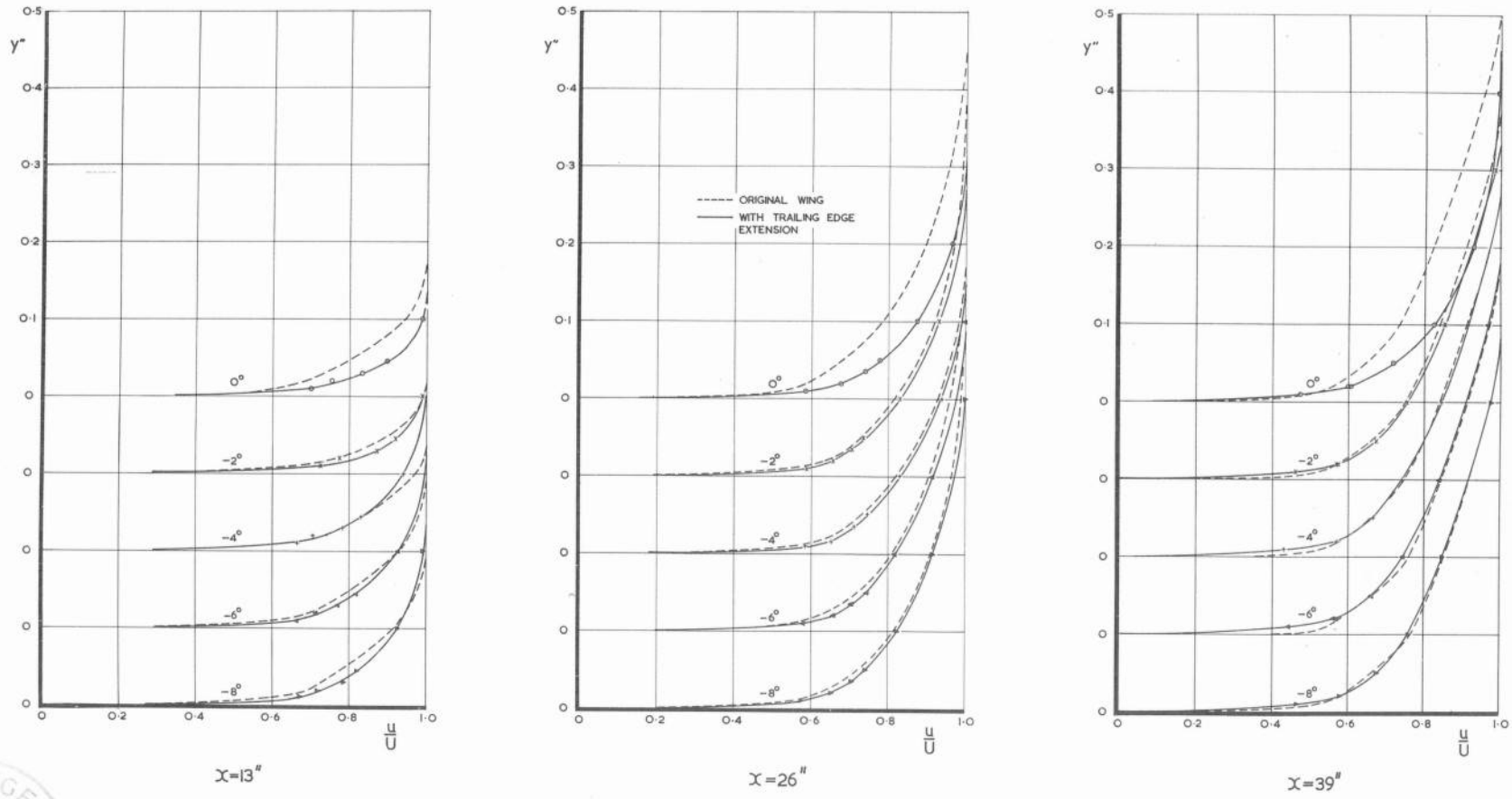

(c) R = 1·08 x 10^6/FT.
α = -8° — 0°

FIG. 11. BOUNDARY LAYER VELOCITY PROFILES. y/s = 0·223

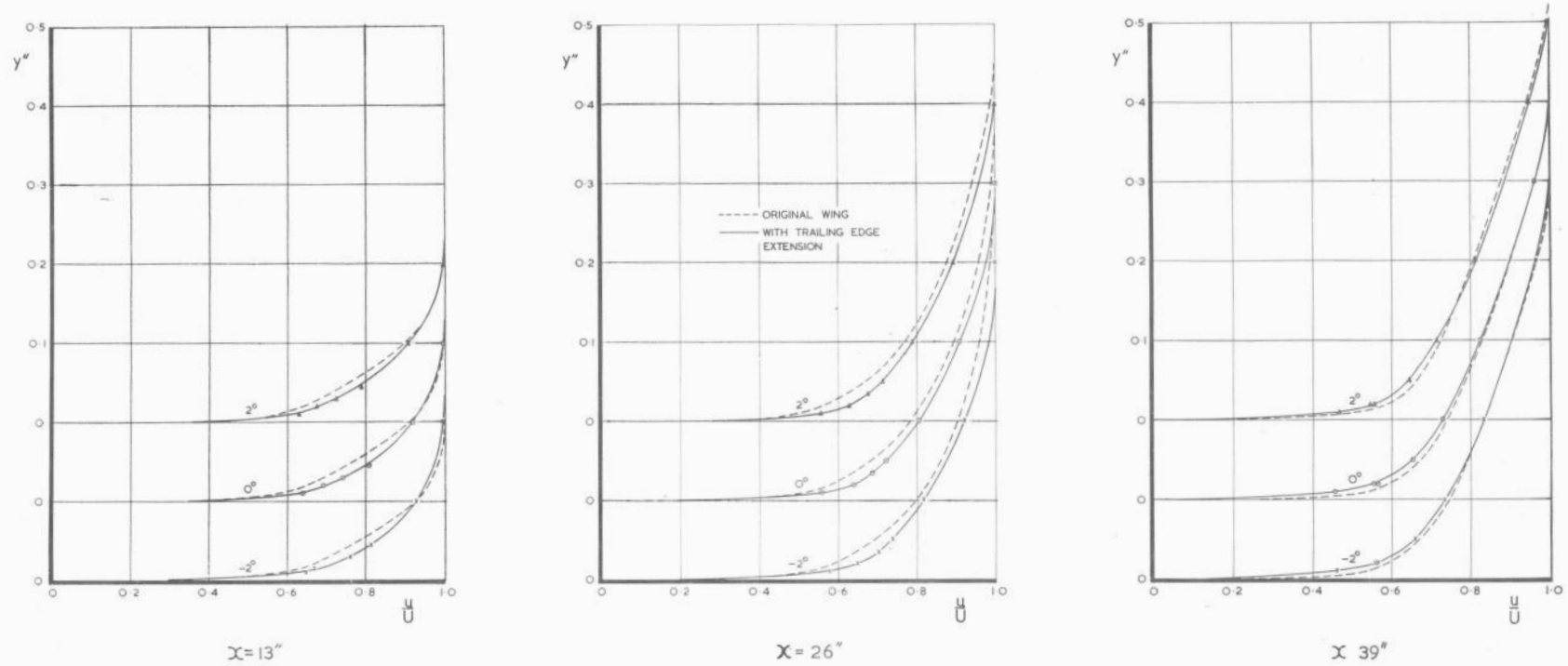

(d) $R = 1{\cdot}55 \times 10^6$/FT.

FIG. 11. BOUNDARY LAYER VELOCITY PROFILES. $y/s = 0{\cdot}223$

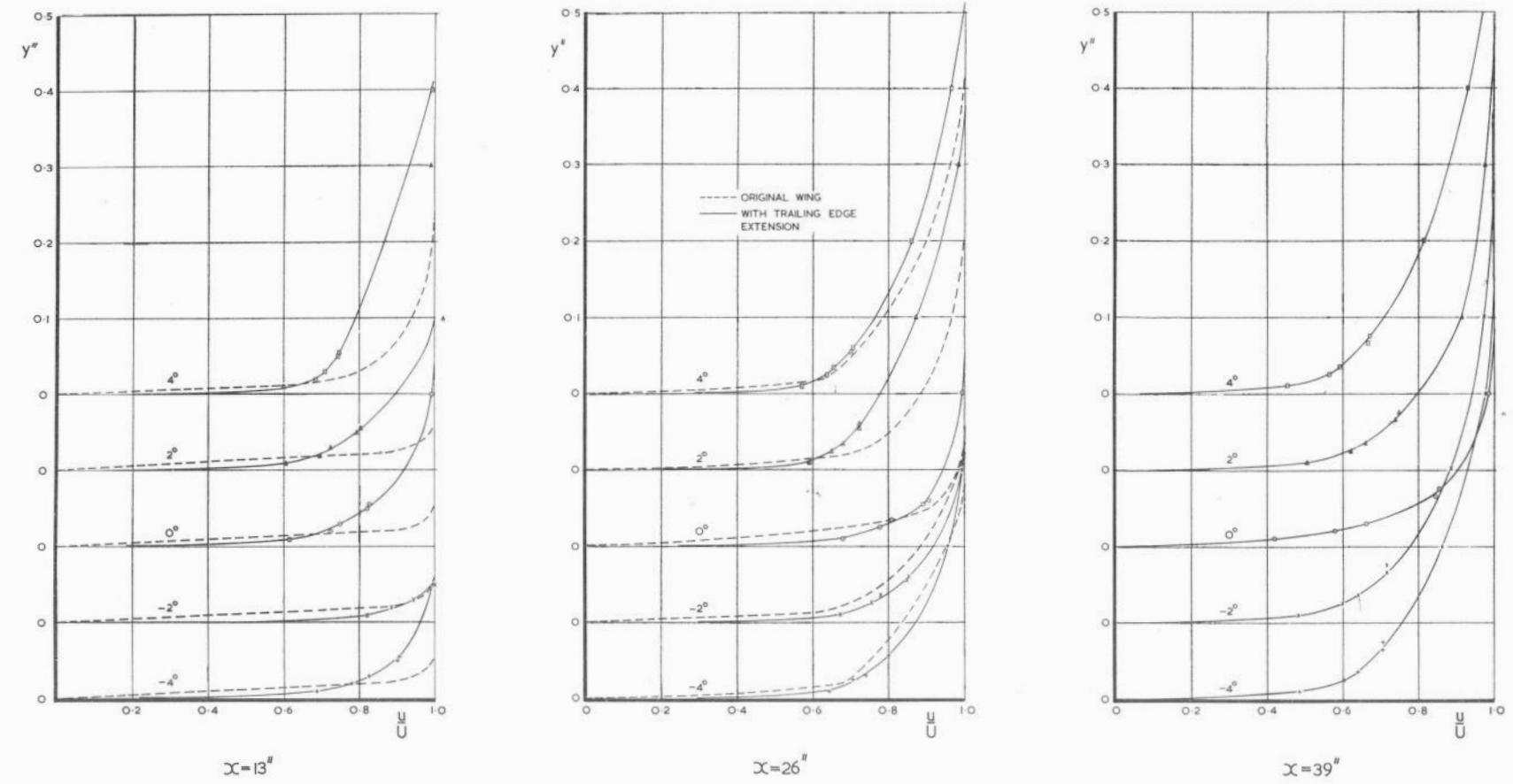

(a) R = 0·88 x 10^6/FT.

FIG. 12. BOUNDARY LAYER VELOCITY PROFILES. $y/s = 0·497$

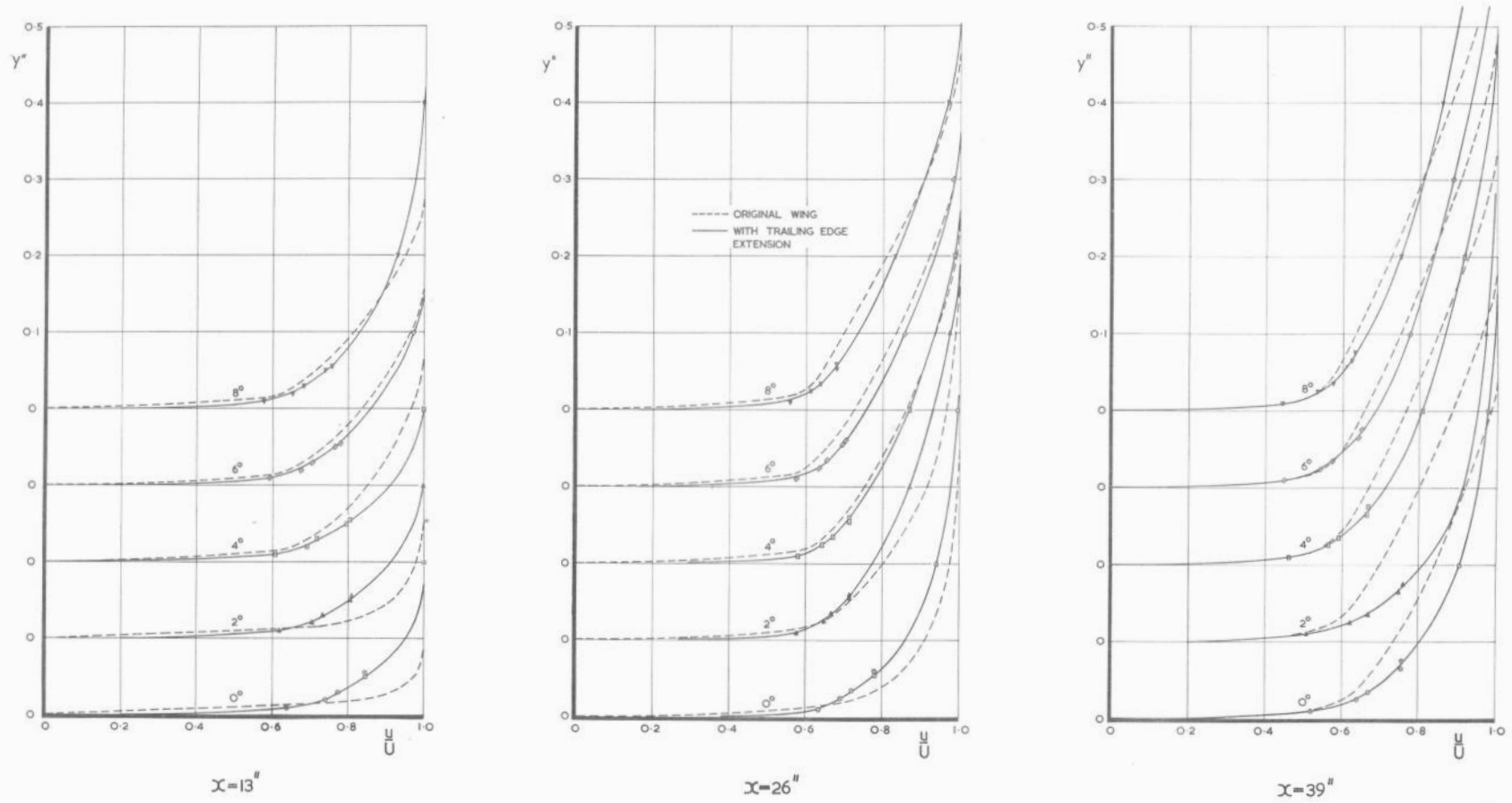

(b) $R = 1{\cdot}08 \times 10^6$/FT.
$\alpha = 0° - 8°$

FIG. 12. BOUNDARY LAYER VELOCITY PROFILES. $y/s = 0{\cdot}497$

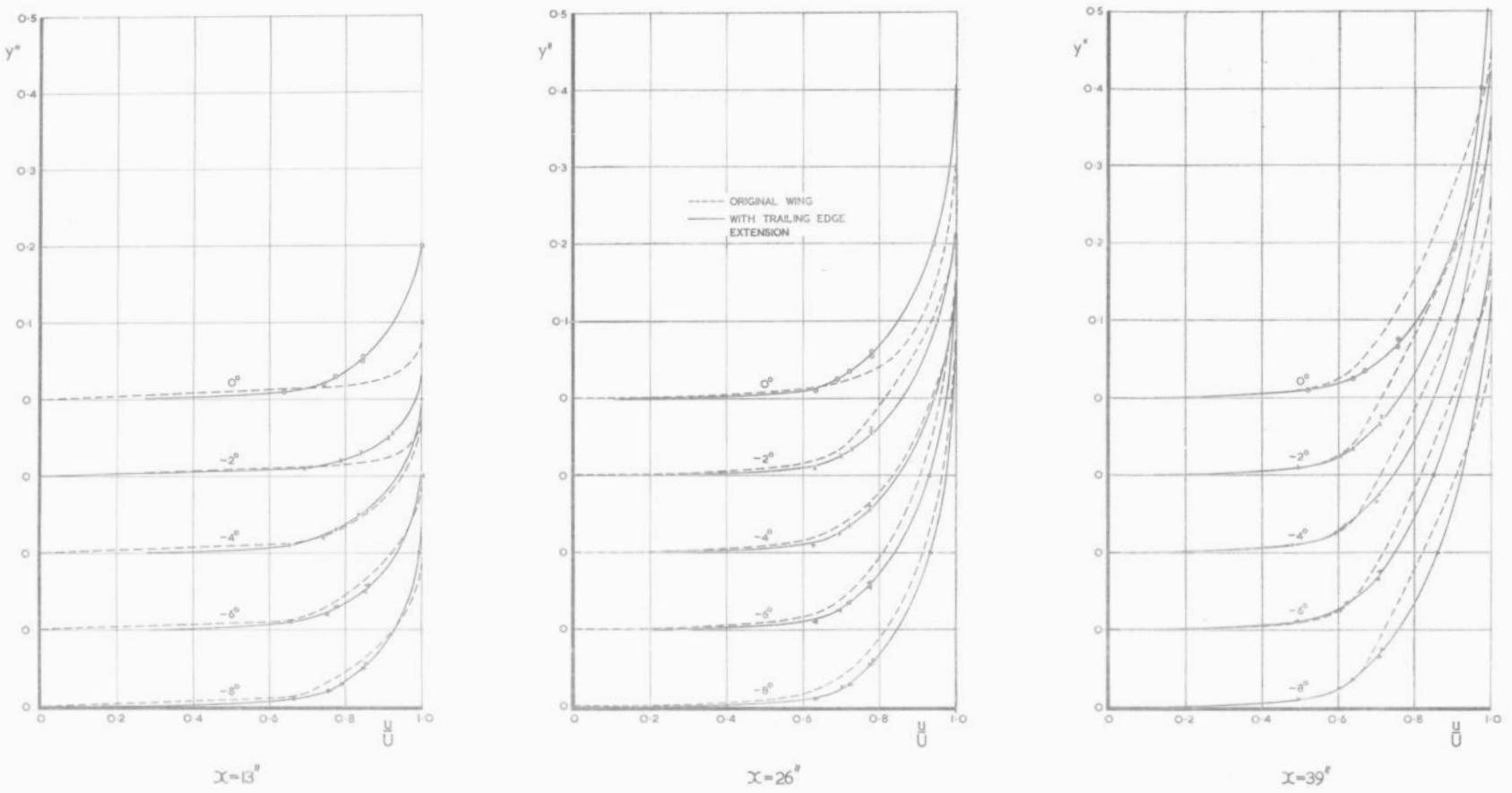

(c) R=1·08 x 10^6/FT.
α = -8° — 0°

FIG.12. BOUNDARY LAYER VELOCITY PROFILES. $y/s = 0{\cdot}497$

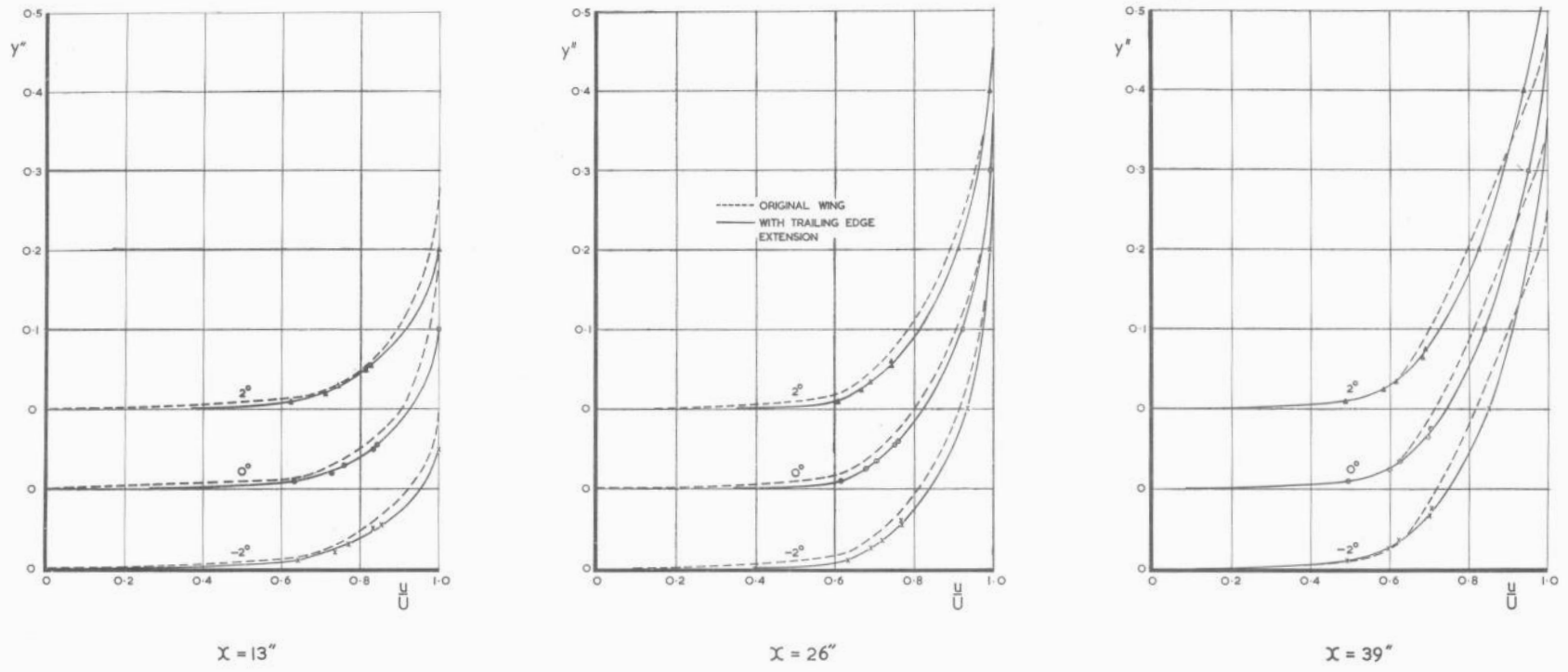

(d) $R = 1{\cdot}55 \times 10^6$ / F.T.

FIG. 12. BOUNDARY LAYER VELOCITY PROFILES. $y/s = 0{\cdot}497$

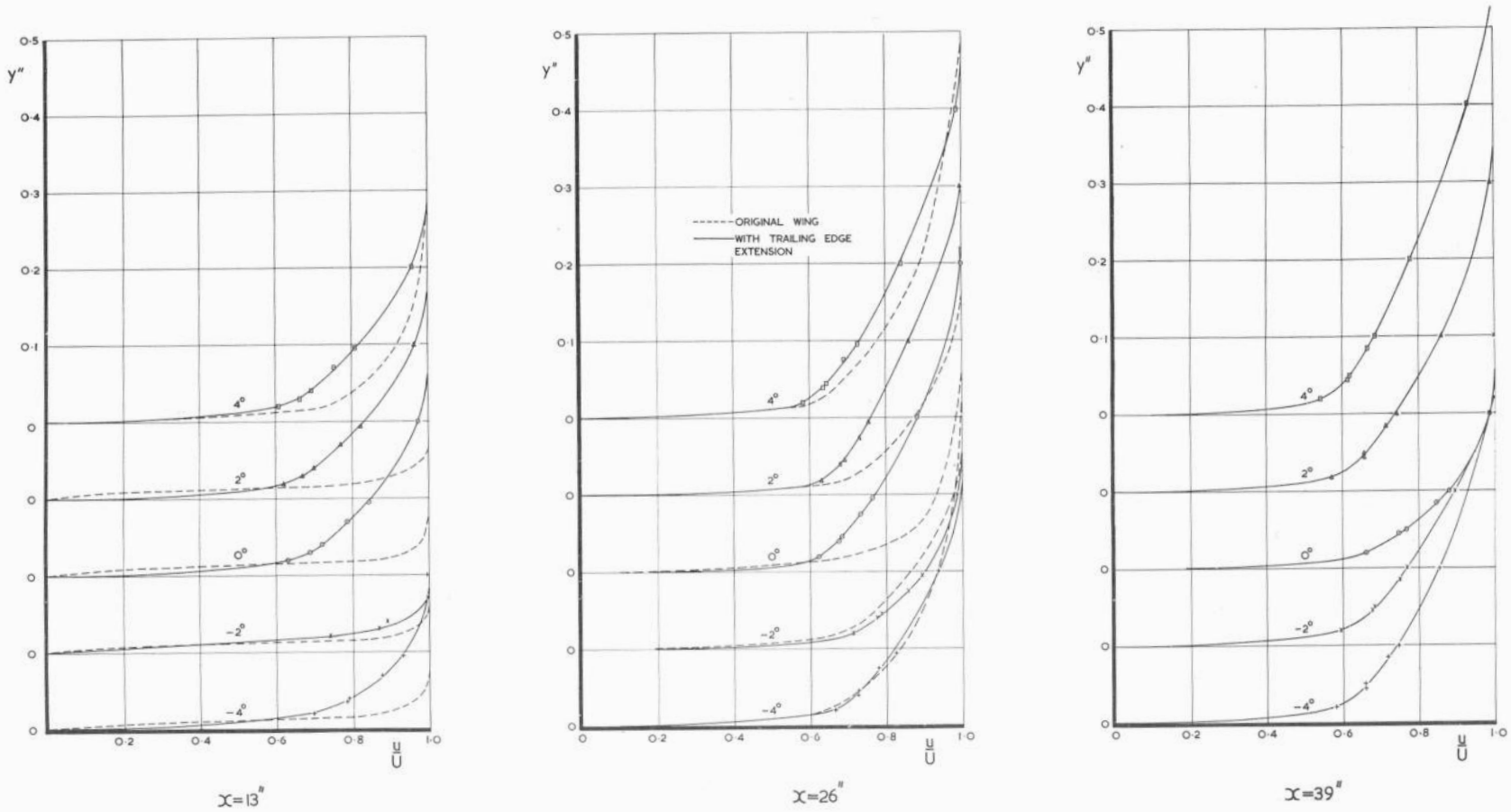

(a) R = 0·88 x 10^6 /FT.

FIG. 13. BOUNDARY LAYER VELOCITY PROFILES. $y/s = 0.772$

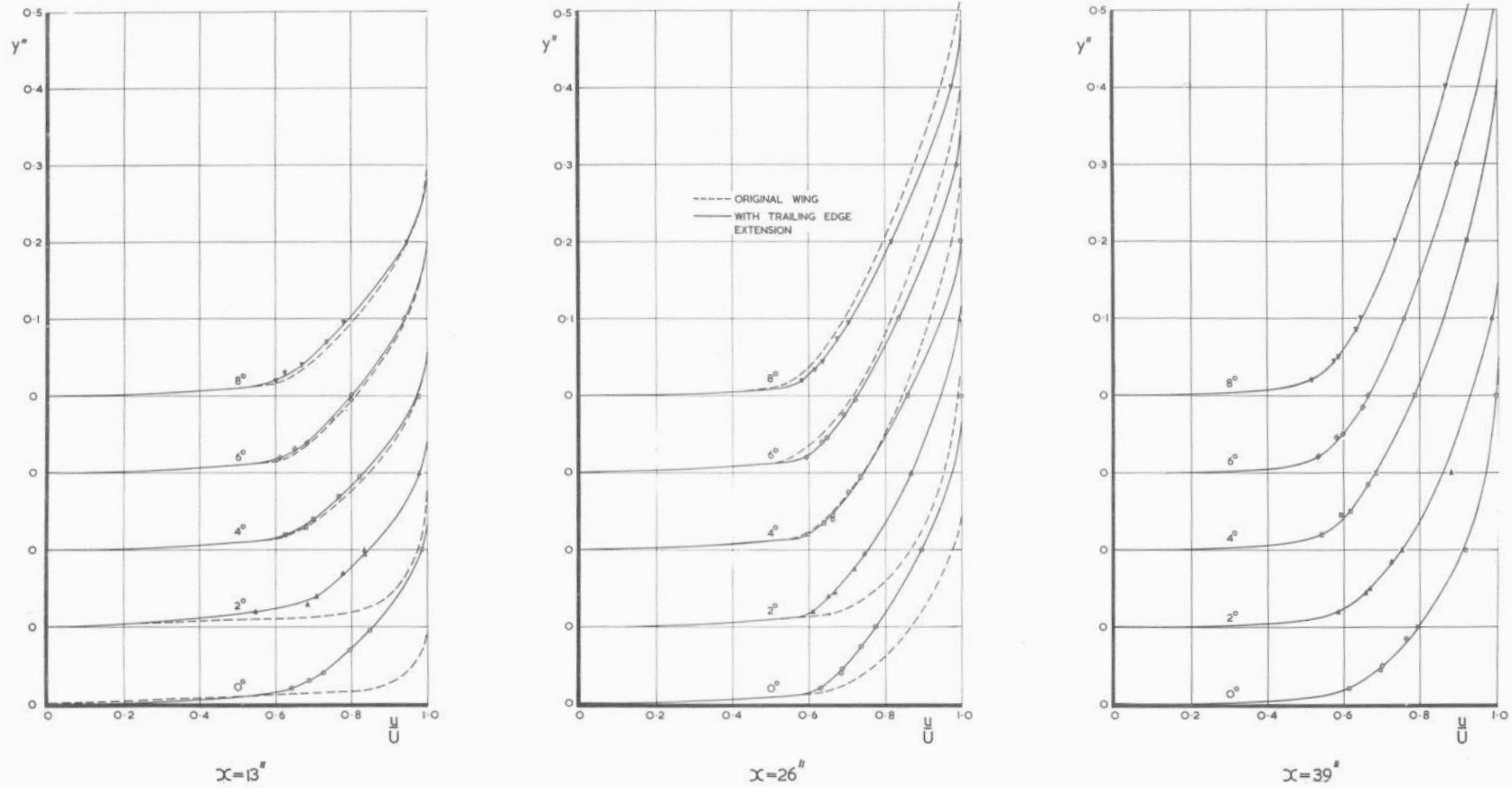

(b.) R = 1·08 x 10⁶/FT.
α = 0°— 8°

FIG. 13. BOUNDARY LAYER VELOCITY PROFILES. $y/s = 0.772$

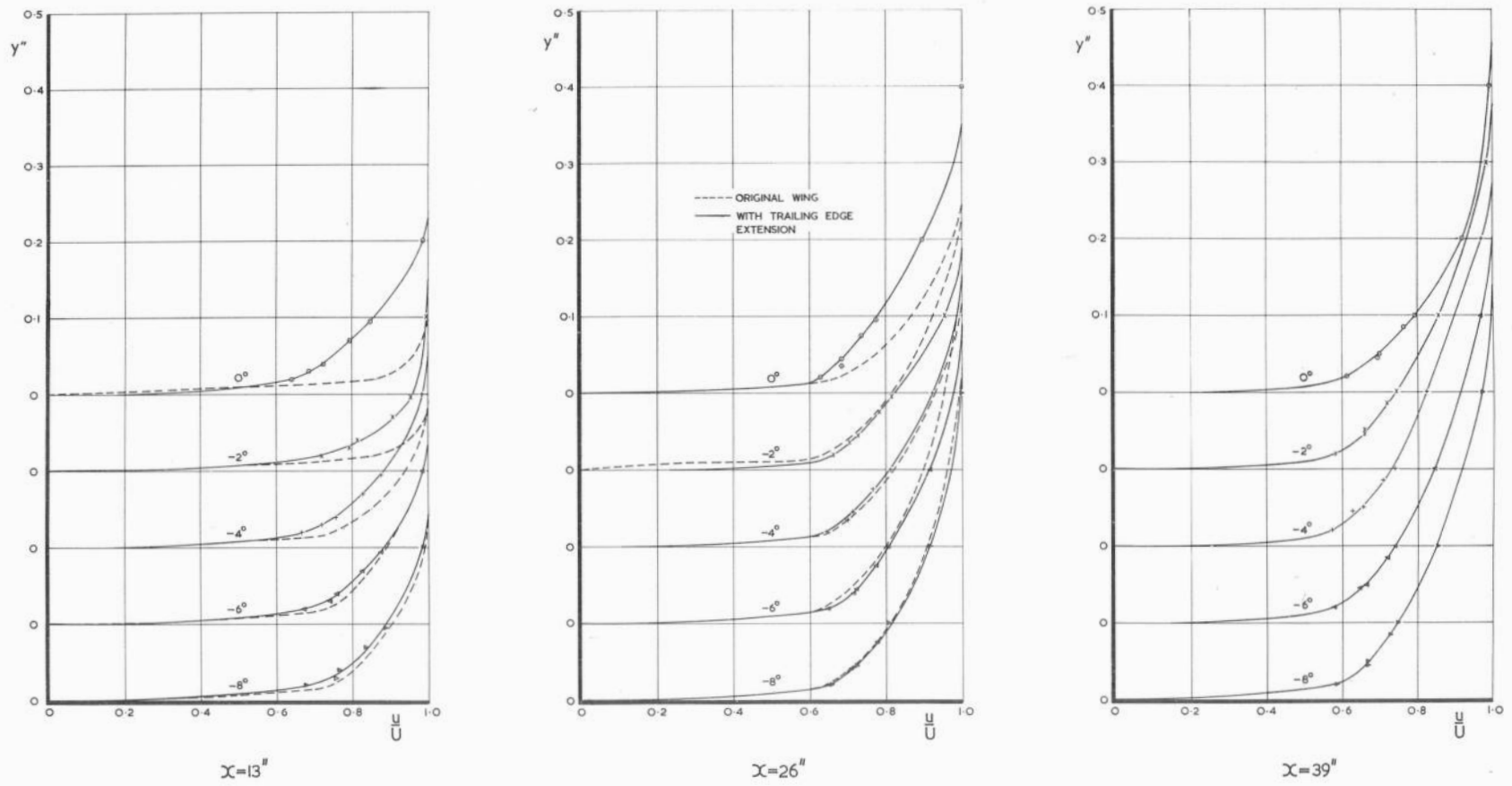

(c) R=1·08 x 10^6/FT.
α = -8° — 0°

FIG. 13. BOUNDARY LAYER VELOCITY PROFILES. $y/s = 0.772$

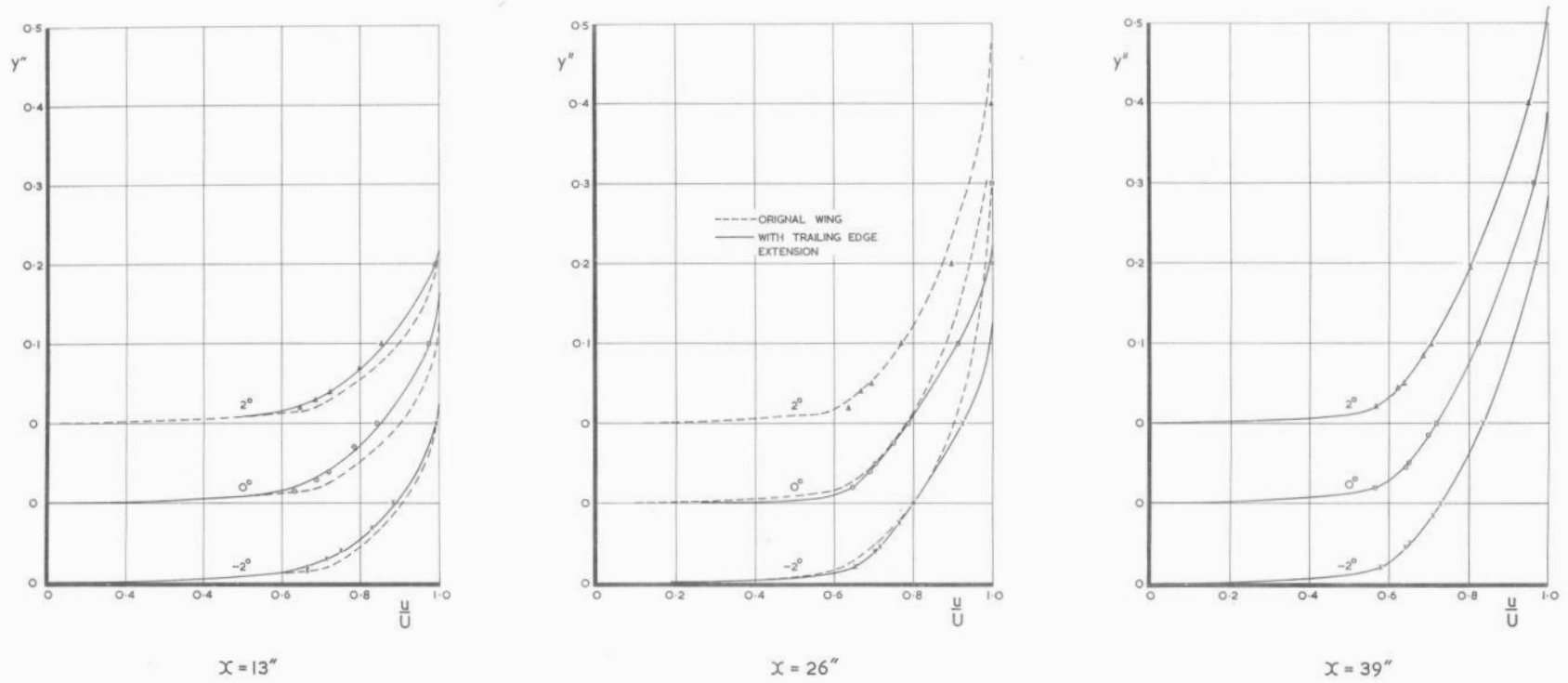

(d) $R = 1{\cdot}55 \times 10^6$ / FT.

FIG. 13. BOUNDARY LAYER VELOCITY PROFILES. $y/s = 0{\cdot}772$

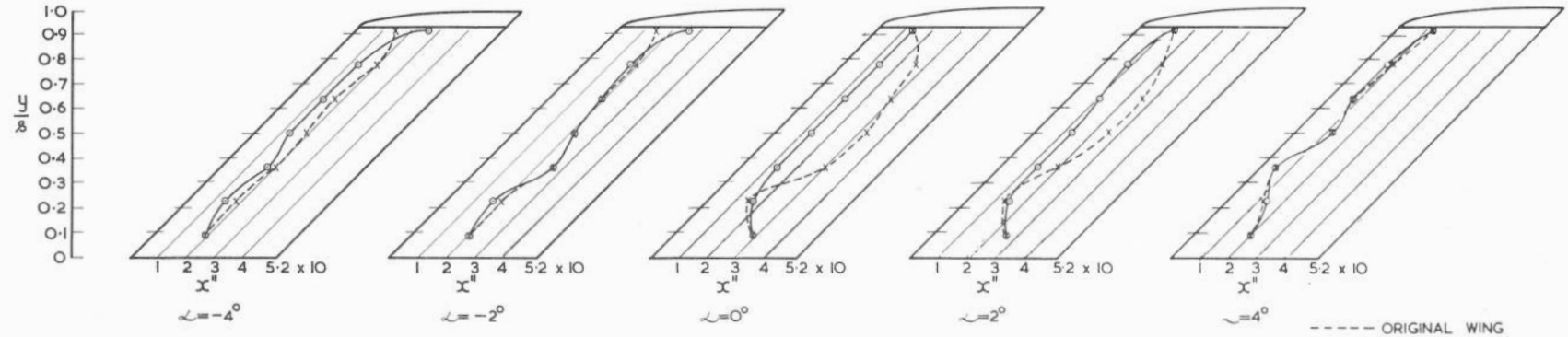

FIG. 14. BOUNDARY LAYER TRANSITION FRONTS. $R = 0{\cdot}88 \times 10^6$ / FT.